Inhibition by CO and Polarization in Pd-Based Membranes: A Novel Permeation Reduction Coefficient

Alessio Caravella,[†] Francesco Scura,[†] Giuseppe Barbieri,*[,†] and Enrico Drioli[†,‡]

National Research Council - Institute on Membrane Technology (ITM-CNR), Via Pietro Bucci, c/o The University of Calabria, Cubo 17C, 87036, Rende (CS), Italy, and The University of Calabria, Department of Chemical and Materials Engineering, Via Pietro Bucci, Cubo 44A, 87036, Rende (CS), Italy

Received: May 25, 2010; Revised Manuscript Received: August 20, 2010

In this Article, a novel permeation reduction coefficient (PRC) is defined and used to take into account the presence of both inhibition by CO and concentration polarization in hydrogen permeation through Pd-based membranes. The usefulness of this coefficient consists in the possibility of describing simply, but at the same time powerfully, the behavior of the membrane subject to the combined effect of inhibition and polarization. According to this approach, the effective permeance, which is generally unknown because it depends on these two phenomena, can be directly evaluated by multiplying the "clean" intrinsic membrane Sieverts permeance (measurable by simple pure hydrogen permeation tests) by a PRC function, that is, [effective permeance] = (1 − PRC) [clean Sieverts permeance]. The values of PRC are evaluated by means of a complex model that takes into account the several elementary permeation steps, in which the inhibitory effect of CO is also considered as well as the concentration polarization. The membrane behavior is evaluated in terms of some "performance maps", where PRC and other two coefficients (concentration polarization coefficient (CPC) and inhibition coefficient (IC)) are reported as functions of several operating conditions (hydrogen molar fraction, CO partial pressure, and upstream total pressures). Therefore, these maps provide a useful tool to estimate directly the main design parameter (the overall permeance) in situations where complex transport and kinetic phenomena affect the membrane performances, allowing the membrane performance to be estimated much better and the separation equipment to be better designed.

1. Introduction

In this decade, the production of ultrapure hydrogen is becoming progressively higher because of the strategic role that hydrogen could play as an energy carrier.[1,2] In fact, a high-purity hydrogen can be used as fuel for feeding the proton exchange membrane fuel cells (PEM-FCs), which can be used for civil and military transport[3] more efficiently than the traditional internal combustion engines and with a much lower impact on the environment. The processes by which hydrogen is mostly produced are essentially represented by oxidation, steam reforming of hydrocarbons, and water−gas shift reaction, which need up-grade stages to lead the hydrogen to reach the required purity, whose level strongly depends on the application for which it has to be utilized. Among the different ways that can be used for purifying hydrogen, membrane-based technology can provide significant improvements with respect to the performances of more traditional techniques, even in terms of volume plant reduction, which is one of the objectives of the Process Intensification Strategy,[4] whose main aim consists of a better exploitation of the raw materials and resources. Among the different types of membranes available to be adopted in reaction and hydrogen separation processes, the Pd-alloy based membranes assume a significant importance because of their peculiarity to be permeable to only hydrogen.[5] Nevertheless, a strong limitation to the massive use of the Pd-based membranes in full-scale chemical plant could be the quite high costs of palladium and its alloys. For this reason, great efforts have been and are still being made to decrease the incidence of the material costs on the overall membrane fabrication by reducing the thickness of the Pd-based selective layer as much as possible, which is deposited on an appropriate support, providing the necessary mechanical resistance. However, as already stressed in several works of the literature (e.g., refs 6−14), when the selective layer is very thin (<5 μm ca.) the membrane performances could be severely reduced because of the concentration polarization. In principle, this phenomenon affects all membrane processes, even though for the gas separation it was neglected for a long time in the past. Its effect on hydrogen purification involving Pd-based membranes has been recently investigated from a modeling point of view by Caravella et al.[7] and experimentally by Peters et al.,[10] who also measured the influence of the CO content in the mixture to purify in terms of reduced membrane performances due to the inhibition phenomenon. Some other authors observed the effects on some superficial modifications induced on the Pd-based surfaces by interfacial reactions,[15−21] which also modify the intrinsic membrane performances by causing a change in the number of superficial active sites. However, these phenomena are not properly related to inhibition because they have also been observed at quite high temperatures.[15]

Concerning the influence of CO on the Pd-based membranes, it is already well known from the literature that CO inhibits the hydrogen capability to permeate through the Pd membranes. In particular, it is generally accepted that the CO−Pd surface bond involves a physical adsorption phenomenon,[22−26] which is favored at low temperatures. Several studies on the performance

* Corresponding author. E-mail: g.barbieri@itm.cnr.it, giuseppe.barbieri@cnr.it. Fax: +39 0984 402103.
[†] National Research Council - Institute on Membrane Technology (ITM-CNR).
[‡] The University of Calabria.

10.1021/jp104767q
Published on Web 09/03/2010

decrease in the Pd membranes and Pd membrane reactors due to inhibition have been carried out.[10,27−29] In these studies, the underestimation of the membrane area caused by neglecting the inhibition by CO in designing a reactor, separation equipment, or both is stressed. In fact, the inhibition phenomenon can be relevant not only in gas separation but also in reactive processes like the water−gas shift,[30] which involves CO as a principal reactant at a relatively low temperature (280−350 °C). From these considerations, it appears necessary to take into account as accurately as possible both polarization and inhibition by CO in hydrogen permeation through Pd-based membranes, which follows the Sieverts law (eq 1) if hydrogen diffusion in the Pd-based layer is the rate-determining step of the whole permeation process.

$$J_{H_2} = \pi^{\text{Sieverts}}\left(\sqrt{P_{H_2}^{\text{retentate}}} - \sqrt{P_{H_2}^{\text{permeate}}}\right) \quad (1)$$

In the case of pure hydrogen permeation tests, the driving force can be evaluated between the fluid bulks or, invariantly, between the membrane surfaces of retentate and permeate because neither inhibition nor polarization affects the system. Therefore, under these conditions, Sieverts permeance π^{Sieverts} is an intrinsic property of the membrane. However, when one or both of these phenomena are present, the bulk properties are generally different from the ones evaluated at the solid−fluid interfaces. Consequently, bulk and intrinsic permeance of membrane can differ appreciably with respect to each other. In this sense, the aim of this Article is the development of a systematic method to account for the presence of both inhibition and polarization by keeping the form of Sieverts law but modifying its structure by means of an appropriate overall permeation reduction coefficient (PRC) (eq 2)

$$J_{H_2} = (1 - \text{PRC})\pi^{\text{Sieverts}}\left(\sqrt{P_{H_2}^{\text{retentate}}} - \sqrt{P_{H_2}^{\text{permeate}}}\right)\Big|^{\text{bulk}} \quad (2)$$

In this equation, whose development and implications will be analyzed in detail throughout this Article, the only quantity necessary to calculate the flux is justly PRC because intrinsic Sieverts permeance (not affected by inhibition or polarization) and bulk driving force are simply evaluated.

This approach is similar to the one followed in a previous work by Caravella et al.,[7] where the only concentration polarization has been considered by defining a concentration polarization coefficient (CPC) to "correct" Sieverts permeance affected by mass transfer resistance. However, in that work, the effect of inhibition was not considered, which was studied in terms of permeance decrease by Barbieri et al.,[28] who modeled Sieverts permeance reduction by using a Langmuir expression. In short, according to the methodology followed in this work, the two approaches of refs 7 and 28 are merged in this Article (eq 2), including an investigation that at the same time considers inhibition by CO and concentration polarization, which were previously separately modeled.

2. Description of the System

The system considered for this analysis is the same as the one described in ref 7. In particular, a tube-in-tube Pd-based membrane permeator is chosen as reference equipment (Figure 1), in which an investigation is performed on what occurs along the radial direction of the generic axially infinitesimal volume,

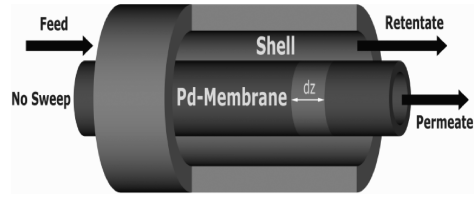

Figure 1. Scheme of a Pd-based membrane permeator in tube-in-tube configuration. The element of the equipment indicated by "dz" identifies the target volume used in Figure 2 for the mass transport analysis.

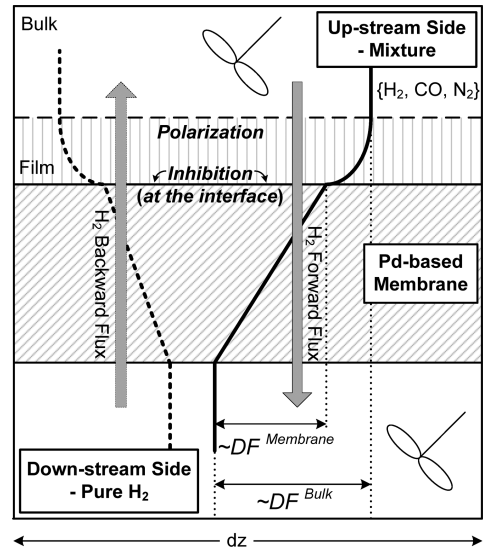

Figure 2. Sketch of the hydrogen permeation in a generic infinitesimal volume of a tube-in-tube permeator (Figure 1). The solid and dashed lines indicate the forward and backward flux, respectively.

whose schematic representation is shown in Figure 2. This sketch shows three different zones: (a) the upstream side, where two mixtures are separately considered; (b) the Pd-based membrane; and (c) the downstream side, where pure hydrogen is present.

Both forward and backward permeation are taken into account in this investigation to analyze the membrane when it behaves as hydrogen purifier (forward permeation) or hydrogen supplier (backward permeation). The whole permeation process is modeled by considering several elementary steps, each of which characterized by its own model equations. The details of such a model can be found elsewhere[6,7] and in the course of this Article, too, where some of these steps have been modified to take into account the presence of an inhibitor species.

Because, as said before, the presence of CO can drastically reduce the hydrogen permeation capability, the membrane behavior is not uniform along the separation equipment, and this nonuniformity becomes stronger as the permeation rate progressively increases. Therefore, the importance of understanding and modeling the inhibition phenomenon in detail is crucial to predicting the overall efficiency of a purification process. The concentrated parameters system sketched in Figure 2 has been considered in this work.

In the Figures introduced in the Results and Discussion section, below the changes of the system in a typical separation process will be indicated by means of thick arrows named "separation paths".

3. Mathematical Approaches

3.1. Modeling of Inhibition by CO. To describe the model used in the present work, it is necessary to recall here some of

TABLE 1: Kinetic Phenomena Affected by Inhibition by CO

phenomenon affected by inhibition	specific rate r_i, $mol_H\ m^{-2}\ s^{-1}$	
adsorption	$r_{adsorption} = \frac{2P_{H_2}^{membrane}}{\sqrt{2\pi M_{H_2} R_g T}} \frac{S_O}{1 + K(\theta_{OO}^{-1} - 1)}$ $\theta_{OO} = 1 - \theta - \frac{2\theta(1-\theta)}{1 + \sqrt{1 - 4\theta(1-\theta)[1 - e^{[w/RT]}]}}$	(3)
desorption	$r_{desorption} = k_D N_S N_{AA} = 2N_S\theta_{AA}$ $\theta_{AA} = \theta - \frac{2\theta(1-\theta)}{1 + \sqrt{1 - 4\theta(1-\theta)[1 - e^{[w/RT]}]}}$	(4)
surface-to-bulk	$r_{surface\ to\ bulk} = \upsilon N_A N_b (1 - \xi)$	(5)
bulk-to-surface	$r_{bulk\ to\ surface} = \beta N_O N \xi$	(6)

TABLE 2: Net Rate of the Kinetic Phenomena Reported in Table 1

permeation step affected by inhibition	specific net rate R_i^{net}, $mol_H\ m^{-2}\ s^{-1}$	
adsorption	$R_{adsorption}^{net} = r_{adsorption} - r_{desorption}$	(3-4)
desorption	$R_{desorption}^{net} = r_{desorption} - r_{adsorption}$	(4-3)
surface-to-bulk	$R_{surface\ to\ bulk}^{net} = r_{surface\ to\ bulk} - r_{bulk\ to\ surface}$	(5-6)
bulk-to-surface	$R_{bulk\ to\ surface}^{net} = r_{bulk\ to\ surface} - r_{surface\ to\ bulk}$	(6-5)

the equations used by Caravella et al.[6] in their paper, That model has been successfully validated under several different operating conditions,[6,7] even in the case of quite high hydrogen concentration (i.e., hydrogen pressure up to 26 bar[7] for a thin Pd-based layers of 2.2 μm). Furthermore, the model is able to deal with high hydrogen concentration (i.e., high pressures) in both the adsorption−desorption kinetics and the hydrogen diffusion through the bulk by means of the secondary terms of the diffusion law. (See ref 6 for details.)

However, despite its complexity, in its original form, such a model is not able to take into account the presence of any inhibitor species affecting the superficial active sites that allow the hydrogen permeation. In this specific case, this analysis starts with considering the model elementary steps that can be affected by an inhibitory effect, that is, the surface phenomena of adsorption and desorption and the two transitions named "surface-to-bulk" and "bulk-to-surface".[33,6] These permeation steps are described by means of expressions (recalled and summarized in Tables 1 and 2) that involve superficial parameters like surface coverage, number of adsorption sites, and so on (more details on them can be found elsewhere[6,31−33]).

These complex expressions contain several variables, whose most important ones related to this analysis are the superficial concentration of the free adsorption sites N_O and of the ones occupied by hydrogen N_A. (By convention, in this notation, the atomic hydrogen is indicated by means of the subscript "A".) The approach adopted in this work is based on the following considerations: the presence of an inhibitor for Pd-based membranes affects the superficial catalytic sites on and from which hydrogen adsorbs and desorbs, essentially by reducing their effective number. Hence, from a macroscopic point of view, the membrane area effectively affected by hydrogen flux is reduced, andhence the permeance, calculated with respect to the nominal membrane area, decreases as well.

This reduction was measured by Barbieri et al.,[28] who provided its quantification at 374 °C by hypothesizing the following Sieverts−Langmuir equation to be valid for the clean permeance reduction

$$\pi_{membrane}^{inhibited} = \left(1 - \alpha \frac{K_{CO} P_{CO}}{1 + K_{CO} P_{CO}}\right) \pi_{membrane}^{clean} \qquad (7)$$

where α and K_{CO} are specific Langmuir temperature-dependent parameters, whose values are reported below in the list of symbols. According to eq 7, the main hypothesis at the basis of the modification proposed in this work consists of assuming that the same reduction law considered for the permeance can also correctly describe the decrease in the superficial concentration of the sites for hydrogen adsorption, which was set as a constant in previous papers.[6,7] In this frame, the use of a quite thick membrane (60 μm) should ensure that the permeation reduction is due to a reduction of the adsorption sites instead of some other superficial phenomena. This fact will be confirmed later in the section of the model validation. Once this reduction has been determined, the model can also be applied to thin membranes.

As a consequence of this reduction, the fraction of the sites occupied by hydrogen (θ) and the empty fraction of free sites available for the hydrogen atomic dissociation ($1 - \theta$) are both reduced with respect to a "clean situation" by the same factor as considered in eq 7, that is

$$1 - \theta = \frac{N_O}{N_S}\left(1 - \alpha \frac{K_{CO} P_{CO}}{1 + K_{CO} P_{CO}}\right), \qquad \theta = \frac{N_A}{N_S}\left(1 - \alpha \frac{K_{CO} P_{CO}}{1 + K_{CO} P_{CO}}\right) \qquad (8)$$

Such modifications are made in the expressions reported in Tables 1 and 2 wherever θ and $(1 - \theta)$ are encountered in the equations. Evidently, the validity of these expressions is strongly related to the hypotheses from which the Sieverts−Langmuir equation was obtained.[28]

After introducing the model, it is now possible and convenient to formalize the definition of an IC, which allows quantifying the clean permeance reduction due to the effect of only inhibition (eq 9)

$$\pi^{\text{inhibited}}_{\text{membrane}}(\text{elementary steps}) = (1 - \text{IC})\pi^{\text{clean}}_{\text{membrane}}(\text{elementary steps}) \quad (9)$$

In these definitions, the expressions "elementary steps" underline the fact that the Sieverts permeance considered in this Article is calculated by means of the complex model already introduced in a previous work[6] and modified here to account for the presence of the inhibition by CO. Examining eqs 7 and 9, it is possible to notice that the coefficient IC is equal to the Langmuir term present in the novel equation.[28] However, the novel equation does not consider the presence of concentration polarization and hence represents just a particular case of the present model, which takes into account the CO partial pressure that is established close to the Pd-based surface, which is generally different from the CO partial pressure of bulk.

$$\text{IC} = \alpha\frac{K_{\text{CO}}P^{\text{membrane}}_{\text{CO}}}{1 + K_{\text{CO}}P^{\text{membrane}}_{\text{CO}}} \quad (10)$$

This coefficient as well as the other two presented in the incoming two sections (CPC and PRC) will be plotted as a function of different conditions to form some "permeation reduction maps", which will be discussed below. The permeances are calculated according to eq 9 and consist of the following procedure: (1) the hydrogen flux is evaluated by taking into account all the permeation steps described in the model; (2) an appropriate process-characterizing driving force is chosen accordingly to the operating conditions; and (3) the permeances (of bulk and membrane) are finally calculated as the ratio of flux and the chosen driving forces (DFs) (of bulk and membrane, respectively).

The "bulk" quantities are the ones evaluated between the bulks of the two membrane sides, whereas the "membrane" quantities are evaluated at the end of the gaseous film responsible of the polarization. Analogously to a previous work,[7] Sieverts DF has been chosen here as the characteristic one of the permeation. Hence, the respective permeances (of membrane and bulk) are calculated as reported in eqs 11 and 12.

$$\pi^{\text{inhibited or clean}}_{\text{membrane}} = \left.\frac{\text{H}_2\text{ flux (elementary steps)}}{\text{DF}^{\text{Sieverts}}_{\text{membrane}} = \Delta\sqrt{P_{\text{H}_2}}\Big|_{\text{membrane}}}\right|^{\text{inhibited or clean}} \quad (11)$$

$$\pi^{\text{inhibited or clean}}_{\text{membrane}} = \left.\frac{\text{H}_2\text{ flux (elementary steps)}}{\text{DF}^{\text{Sieverts}}_{\text{bulk}} = \Delta\sqrt{P_{\text{H}_2}}\Big|_{\text{bulk}}}\right|^{\text{inhibited or clean}} \quad (12)$$

In these expressions, Sieverts DF of membrane is also calculated by the model, whereas Sieverts bulk DF is set according to the external operating conditions. It is very important to highlight that these two permeances can be evaluated in both the presence and the absence of inhibition (as indicated by the superscripts). By convention, when in this Article a permeance is calculated under conditions not affected by inhibition, it is indicated by not using any superscript.

Another important aspect is that according to this approach the inhibition phenomenon could affect the Sievert-wise character of the permeation only at a very high level of superficial occupancy by CO, that is, at a low temperature (<270 °C ca.), and, at the same time, at high inhibitor partial pressure (CO in this case). For a temperature higher than about 280−300 °C, which is the lower limit of the usual usage for the Pd-based membranes, the adsorption and desorption kinetics are very fast[6,33] and almost independent of the surface reduction because of the coverage by CO. Therefore, under these conditions Sieverts law continues to be valid because the "clean" portions of the surface do not perceive the effect of the "inhibited" ones.

3.2. Recall on the Concentration Polarization Coefficient. Because the topic of this Article is analyzing the permeation reduction caused by both polarization and inhibition, it is necessary here to recall the definition of the CPC, already introduced in a previous work.[7] However, as will be shown, such a definition of CPC can also be used to describe situations in which several transport and kinetic phenomena involved in the permeation process are affected by inhibition phenomena. This can be simply done generalizing the previous CPC definition (reported here in eq 13) by evaluating CPC in a situation affected by inhibition (eq 14).

$$\pi_{\text{bulk}}(\text{elementary steps}) = (1 - \text{CPC}|_{\text{old}})\pi_{\text{membrane}}(\text{elementary steps}) \quad (13)$$

$$\pi^{\text{inhibited}}_{\text{bulk}}(\text{elementary steps}) = (1 - \text{CPC})\pi^{\text{inhibited}}_{\text{membrane}}(\text{elementary steps}) \quad (14)$$

In this way, when no inhibition acts on the system, the two definitions are in fact coincident. Furthermore, such a definition ensures that the only influence of external mass transfer is evaluated in this coefficient, allowing the effect of the polarization to be split from the inhibition one, which is measured by means of the IC already defined in the previous section.

3.3. Definition of the Overall Permeation Reduction Coefficient . In this section, an indicator to evaluate directly the permeance loss under several conditions is introduced. In particular, an overall PRC is defined, taking into account the permeation reduction owing to both inhibition and polarization. By analogy to what was done for CPC and IC, PRC is defined by eq 2 and calculated as the ratio of the bulk permeance affected by inhibition and polarization and the one of membrane not affected by inhibition (eq 15).

$$\text{PRC} = 1 - \frac{\pi^{\text{inhibited}}_{\text{bulk}}(\text{elementary steps})}{\pi^{\text{clean}}_{\text{membrane}}(\text{elememtary steps})} \quad (15)$$

This definition arises from the consideration that the bulk permeance in the presence of both inhibition and polarization is the smallest permeance that one can measure, whereas, on the contrary, the membrane permeance with no external influence is the maximum one that a user wants to exploit as much as possible. By combining eqs 9, 13, and 15,

TABLE 3: Summarization of the Reduction Coefficients Considered in This Work

coefficient	formal definition	mathematical definition
CPC	concentration polarization coefficient	$\pi_{bulk}^{inhibited} = \pi_{membrane}^{inhibited}(1 - CPC)$ (17)
IC	inhibition coefficient	$\pi_{membrane}^{inhibited} = \pi_{membrane}^{clean}(1 - IC)$ (18)
PRC	permeation reduction coefficient	$\pi_{bulk}^{inhibited} = \pi_{membrane}^{clean}(1 - PRC)$ (19)

TABLE 4: Different Scenarios Described by PRC

permeation reduction coefficient	equivalent reduction coefficient	phenomena involved in
PRC =	0	neither inhibition nor polarization
	IC	only inhibition
	CPC	only polarization
	PRC	both inhibition and polarization

it is possible to express PRC in terms of IC and CPC (eq 16)

$$PRC = 1 - (1 - CPC)(1 - IC) \quad (16)$$

This relation clearly shows the nonlinear dependence of PRC on IC and CPC, which means that in terms of permeance, the effects of polarization and inhibition should not be simply added to each other. The summary of the reduction coefficients introduced in this Article is reported in Table 3. The usefulness of this approach consists of the fact that the so-defined PRC is able to describe the four possible scenarios (summarized in Table 4) in which the system can be found: (1) Neither polarization nor inhibition phenomena are present. In this case, there is no permeation reduction, and hence PRC is zero as well as CPC and IC. (2) Only inhibition affects the membrane. In this case, the only permeation reduction is due to the inhibitors present, and thus PRC and IC coincide. (3) Only polarization reduces the membrane permeance. Differently from the previous case and for analogous reasons, in this situation, PRC is equal to CPC. (4) Both phenomena act on the system; therefore, the contributions of both CPC and IC are taken into account.

4. Results and Discussion

The innovative results of this work are introduced and discussed in three different subsections, in the first of which the experimental validation of the analysis (by means of the literature data) is provided. Then, the inhibition and polarization influence on the membrane considered is shown in terms of reduced hydrogen permeance and permeating flux. Finally, the system behavior is analyzed in terms of the novel coefficients defined and presented in the previous sections.

4.1. Validation of the Model. In this section, a confirmation of the present approach is provided. It must be underlined that this is an extension of the model already introduced in previous works[6,7] with the corresponding experimental validations under both pure hydrogen and mixture tests (concentration polarization study).

4.1.1. Experimental Data from Barbieri et al.[28] The first set of experimental data considered for validation is taken from Barbieri et al.[28] As described in the previous section, the same functionality of the permeance reduction considered in ref 28 has been introduced in the complex model described in refs 6 and 7 to take into account the reduction of the number of adsorption sites due to CO inhibition. The results of this investigation are shown in Figure 3, where the curve related to the novel equation[28] (dashed line) is also reported for comparison. Before commenting on these results, it is necessary to explain how the curve of the present model was obtained. First, the kinetic parameters of hydrogen diffusion coefficient through the palladium lattice (whose expression and results are reported in eq 20, Table 5) were calculated from the pure hydrogen permeation tests at different temperatures by means of a nonlinear regression of the model.

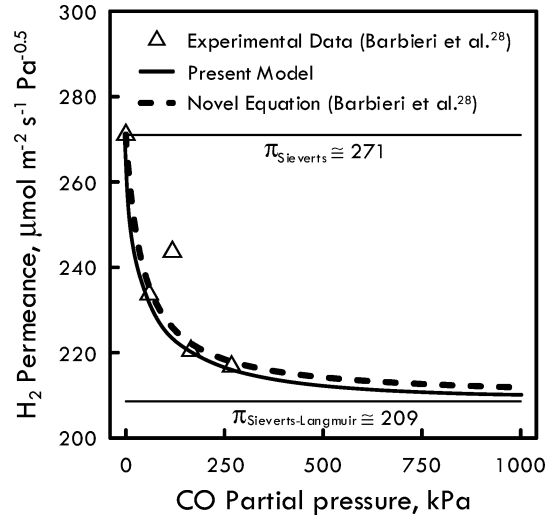

Figure 3. Comparison between present model, experimental data and novel equation (Barbieri et al.[28]) in terms of hydrogen permeance as a function of hydrogen composition of the upstream mixture. A mixture (H_2, CO) was used in the experiments at a constant H_2 partial pressure in retentate (150 kPa), 374 °C, and membrane thickness = 60 μm.

TABLE 5: Parameters of the Diffusion Coefficient of Atomic Hydrogen through Palladium-Based Lattice of the Membrane of Barbieri et al.[28]

$$D_H = D_H^0 \exp\left(-\frac{E}{R_g T}\right) \quad (20)$$

D_H^0, m^2 s^{-1}	E_d, J mol^{-1}
9.45×10^{-8}	14 175

Afterward, the permeance reduction law was applied to the superficial number of sites on the Pd surface, as reported in Section 3.2. Therefore, the first experimental point shown in Figure 3 (corresponding to the pure hydrogen value) is needed only to characterize the physical properties of the membrane and hence cannot be used to check the predictive ability of the model.

On the contrary, the other points, corresponding to permeation tests with inhibition by CO, can be used to predict the model goodness because exactly the same Langmuir "reduction" law parameters as the ones obtained by Barbieri et al.[28] were used in the calculation. As it is clearly demonstrated in Figure 3, the accordance between the present model (solid line) and experimental results is very good, except for the third point located at ~120 kPa for the relatively anomalous value of which the same authors do not provide any explanation.[28]

In this Figure, the curve of the novel equation (dashed line) is also reported for comparison. Looking at the plots, it must be underlined that although the difference between these two curves is very small, they have to be read in a different way. In fact, the characteristic parameters of the novel equations were calculated by means of the reported experimental data, whereas the present approach used those data to provide an interpretation of those data on a microscopic level. In other words, the two curves are obtained by a different methodology: the one from Barbieri et al.[28] arises from an experimental evaluation of the two parameters of the Langmuir law, whereas the other one is built by calculating the overall permeance by means of a complex model. Therefore, the fact that they are close to each other confirms the goodness of their determination. In this sense, the most important aspect to be highlighted at this point is that microscopic (superficial properties of the Pd-alloy) and macroscopic (permeance, for example) parameters have been linked each other in such a way that the first ones can be directly obtained from the second ones.

In this particular case, this has been possible because the membrane is quite thick and it is reasonably sure that the diffusion of atomic hydrogen in the selective layer is the rate-determining step. If the membrane had not been sufficiently thick, then other mechanisms could have been slow enough to provide a significant influence, and thus the diffusion parameters estimation procedure could have become inconsistent and its results devoid of significance. Therefore, the here-reported analysis clearly demonstrates the nontrivial fact that the permeance reduction is due to a reduction of the adsorption sites that follows the Langmuir-type law. Consequently, this permits one to give the parameters of the novel equation in ref 28 a more specific meaning, which is related not just to a permeance reduction (macroscopic level) but rather to a morphological property of the membrane (adsorption/desorption surface area).

4.1.2. Experimental Data from Mejdell et al.[17] The other set of experimental data is obtained from the work of Mejdell et al.,[17] who investigated the inhibition by CO and also CO_2 on hydrogen permeation through a very thin membrane (3.3 μm ca.) at different temperatures. This work was selected because the particular microchannel configuration used in the permeation tests allows the concentration polarization effect to be minimized,[17] permitting in this way the intrinsic CO influence on the Pd-based surface to be caught. The original experimental data are provided in the form of normalized hydrogen flux as a function of the CO partial pressure. A three-component mixture was considered in the feed side (H_2, N_2, and CO), keeping a constant feed hydrogen molar fraction (0.9) and changing appropriately the CO partial pressure. Total feed and permeate pressure were kept to 300 and 100 kPa, respectively, with argon used as sweep gas. To validate the model, we preliminarily evaluated the specific diffusion kinetic constants (eq 20) and inhibition parameters (eq 7), similarly to what was done in the previous section. The inhibition parameters were estimated for all temperatures considered by Mejdell et al.[17] by a nonlinear regression of the eq 7, which was conveniently re-elaborated in the form expressed by eq 21

$$1 - \frac{J_{H_2}}{J_{H_2}^{clean}} \frac{\Delta P_{Sieverts}^{clean}}{\Delta P_{Sieverts}^{inhibited}} = \alpha \frac{P_{CO}}{K_{CO}^{-1} + P_{CO}} \qquad (21)$$

The ratio of Sieverts driving forces under "dirty" and "clean" conditions (with and without CO, respectively) arises because the hydrogen partial pressure changes during the experimental tests. Therefore, it takes into account that the decrease of flux is due to both presence of CO and the reduction of hydrogen partial pressure in upstream, which decreases when the CO partial pressure is augmented.

TABLE 6: Parameters of the Novel Equation 28 at Different Temperatures Estimated from the Data of Mejdell et al.[17]

diffusional parameters (eq 20)	D_H^0, $m^2\ s^{-1}$	E_d, J mol^{-1}
	1.28×10^{-7}	18 603
inhibition parameters (eq 7)		
T, °C	α	K_{CO}, Pa^{-1}
275	0.9367	0.0124
300	0.8989	0.0063
325	0.8329	0.0032
350	0.7504	0.0014

The results of such evaluation are reported in Table 6, where the values of the inhibition parameters of the novel equation are reported for several temperatures. The value found for the activation energy indicates that the hydrogen metal bulk diffusion is the rate-determining step even at such low thickness (3.3 μm), because the surface phenomena are usually characterized by a higher activation energy.[33,34] By introducing such parameters in the previously recalled complex model, a comparison between experimental and simulation data can be made (Figure 4).

The good accordance shown in the Figure for all temperatures considered confirms that the model is able to represent well the Pd-based membrane behavior in the presence of CO. This aspect becomes more significant if considering the fact that such a model is also able to describe the effect of the concentration polarization on hydrogen permeation. In fact, thanks to this peculiarity, these two phenomena (inhibition and polarization) can be coupled for the first time and analyzed in detail by separating their respective contributions on the flux reduction, as described in the next section.

It has to be recalled here that a theoretical functionality of the inhibition parameters with temperature is out of the aims of this work, and hence only a single temperature (374 °C) with the corresponding inhibition parameters is considered in the following analysis. (See Section 4.1.1.)

4.2. Influence of Inhibition and Polarization on Permeance and Flux. Once the model validation has been provided, in this section both separated and combined effect of

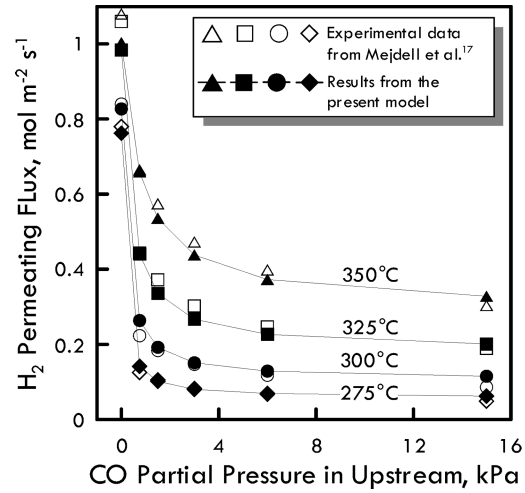

Figure 4. Comparison between present model and experimental data from Mejdell et al.[17] The empty and full symbols indicate experimental data and model results, respectively. $P^{upstream} = 300$ kPa ($H_2 + N_2 + CO$), $P^{downstream} = 100$ kPa ($H_2 + Ar$). membrane thickness = 3.3 μm.

TABLE 7: Operating Conditions Used in the Simulation

	molar fraction							
	mixture 1			mixture 2				
side	H_2	CO	N_2	H_2	CO	N_2	total pressure, kPa	fluid dynamic conditions
upstream	{0, ..., 1}	{0, ..., 0.5}	{0, ..., 0.5}	{0, ..., 1}	{0, ..., 1}		{400, ..., 1000}	$Re \approx 1200$
downstream	1			1			200	not influent

temperature = 374 °C; membrane thickness = 60 μm

TABLE 8: Values of the Diffusion Coefficient Calculated in Some Operating Conditions Considered in This Work[a]

	binary diffusivity coefficients, $m^2\ s^{-1}$		
total pressures, kPa	H_2-N_2	H_2-CO	N−CO
400	6.96×10^{-5}	7.04×10^{-5}	1.93×10^{-5}
600	4.64×10^{-5}	4.70×10^{-5}	1.28×10^{-5}
800	3.48×10^{-5}	3.52×10^{-5}	0.96×10^{-5}
1000	2.78×10^{-5}	2.82×10^{-5}	0.77×10^{-5}

[a] $T = 374$°C.

inhibition and polarization are analyzed as functions of upstream mixtures composition and total pressure. For the reason explained in the previous section, the investigation is carried out at the fixed temperature of 374 °C.

To distinguish the CO contribution to polarization and inhibition, two mixtures are considered: mixture 1, with hydrogen, carbon monoxide and nitrogen (inert for the Pd-based surfaces), and mixture 2, with only hydrogen and carbon monoxide. A summary of these different operating conditions is reported in Table 7. Furthermore, the binary diffusion coefficients calculated under some operating conditions are reported in Table 8. In Figure 5, the hydrogen permeance is reported as a function of the hydrogen molar fraction for the two mixtures. The thick arrows drawn on the curves indicate the typical paths, followed by the system during a membrane separation process, that is, from a high to a low content of the species to recover (hydrogen in this case). The behavior of the system in the two mixtures is qualitatively the same. In this Figure, several situations are analyzed: (1) permeation without external effects owing to polarization or inhibition by CO; (2) permeation with only polarization, where the surface inhibitor interaction of CO has been neglected; (3) permeation with only inhibition by CO (no polarization effect is considered); and (4) the overall situation where permeation with the effect of both polarization and inhibition is examined.

In the first case (horizontal dashed lines), the membrane permeance is constant because it is an intrinsic property of the material not influenced by any external fluid-dynamic factor. When the polarization effect is taken into account (second case), the permeance measured by considering the bulk driving force (indicated with the increasing dashed line named "bulk" in the Figure) differs significantly with respect to that of the membrane. This occurs because of the effect of the external mass transfer, whose resistance is progressively higher as the content of the other species increases. Therefore, the gap between the membrane and bulk permeance is a measure of the polarization level, whose extent will be later quantified by the CPC according to the definition reported in eq 14. An analogous result has been also obtained in a previous work.[6]

The third case analyzed concerns the presence of inhibition only by CO (without polarization), indicated in the Figure by the upper continuous line. Differently from the concentration polarization, the inhibition directly affects the catalytic property of the membrane surface owing to the presence of an inhibitor species blocking the active superficial sites on which the hydrogen molecules dissociates. It is necessary here to highlight that in this case the property being affected by inhibition is the intrinsic membrane permeance and not the apparent (bulk) one.

As said in Section 3.2, this is an equilibrium phenomenon, which has been modeled by means of a Sievert−Langmuir approach, according to which the inhibition approaches toward a constant level and reaches a plateau as the CO partial pressure goes to infinity. This is the reason for the different behavior shown by the permeance affected by polarization and the one influenced by inhibition. Also, in this third case, the gap between the membrane permeance with no inhibition and the one with inhibition represents a direct quantification of this phenomenon. The last case takes into account at the same time the influence of both polarization and inhibition. Following the two continuous curves (evaluated in presence of inhibition by CO) from the pure hydrogen case on, it is possible to notice that at the beginning (i.e., hydrogen molar fraction less than about 0.9) there is no appreciable difference between pure inhibition and inhibition affected by polarization. This occurs because the presence of the other species (both CO and N_2 for mixture 1 and only CO for mixture 2) is not important enough to provide significant polarization effect. However, the CO presence strongly affects the membrane performance (flux and permeance) as regards the inhibition phenomenon, which is the most important one toward the high purity zone of the Figure. As the content of the other species increases, the polarization effect becomes progressively more effective, whereas the contribution of inhibition approaches toward the equilibrium value.

At this point, it is necessary to specify and highlight that CO and, in general, all inhibitors, has a double effect on the system: one related to the polarization and one related to the inhibition. This aspect is clearly evidenced when examining the right part of Figure 5, corresponding to mixture 2. An important difference between these phenomena is that the concentration polarization depends on the molar fraction of the nonpermeating species, whereas the inhibition is related to the partial pressure of the inhibitor species. For this reason, when experimental permeation tests are carried out for a binary mixture H_2-CO, the deviation of the membrane behavior from the typical Sieverts law is to be ascribed to inhibition as well as to the polarization. The weights of the two contributions strictly depend on the operating conditions and are evaluable only by means of a model that takes into account both the effects. In this particular case, the zones in Figure 5 where each contribution prevails are recognizable for both mixtures by looking at the slope of the curve that accounts for both the effects. In fact, in the part of low hydrogen molar fraction, its slope is similar to the one of the bulk permeance without inhibition, whereas it is similar to the sole

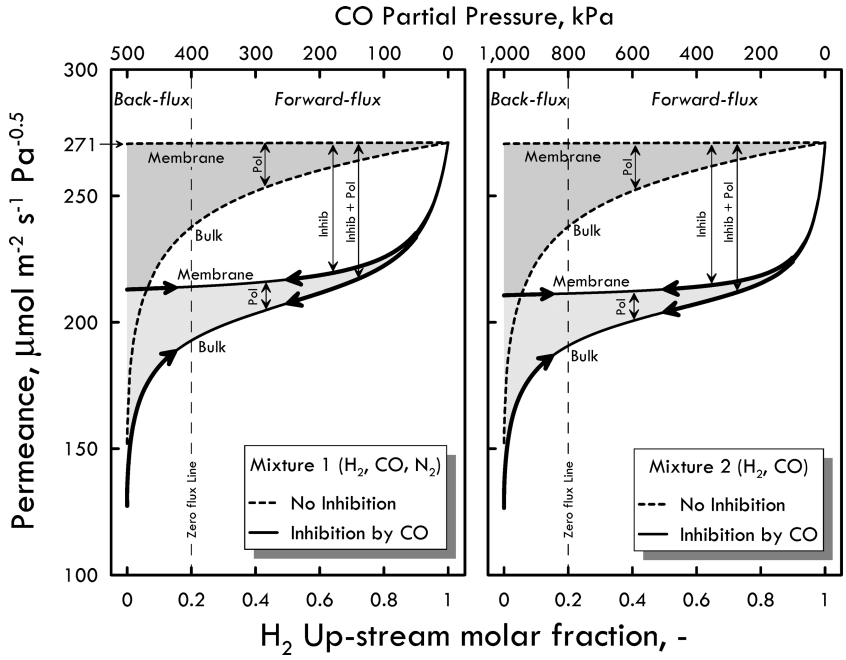

Figure 5. Hydrogen permeances of bulk and membrane as functions of H_2 upstream molar fraction for both mixtures. $P^{upstream} = 1000$ kPa and $P^{downstream} = 200$ kPa. The other operating conditions are reported in Table 7.

inhibition curve. However, another important aspect has to be taken into account: the polarization contributes to increasing the inhibition effect because during the hydrogen permeation, the inhibitor species is "polarized" toward the membrane surface, which, therefore, is subjected to a higher CO partial pressure than the one present in the bulk. This situation can be examined in terms of hydrogen flux (Figure 6) under the same conditions as those considered in Figure 5. Analogously to what was seen for the permeance, in this case, the two mixtures present a quite similar behavior. Examining the forward flux case, the flux with only polarization is higher than that with only inhibition, both being naturally higher that the flux accounting for the two contributions. In the back-flux case, a different situation occurs, presenting an inhibition and polarization fluxes that significantly differ from each other only up to a hydrogen molar fraction of about 0.03, being both practically the same from this value up to the zero-flux line. This occurs because the inhibitor effect of CO has a smaller effect when it affects the membrane surface exposed to low hydrogen partial pressure, where, in the case of back-flux, the hydrogen dissociative desorption is not influenced much by the superficial CO occupancy degree. Furthermore, this is the reason why at the same permeation driving force the back permeation provides higher fluxes than in the forward permeation in the case of only inhibition.

In this case, the back-flux encounters in its path first the membrane resistance and then the one offered by the mixture

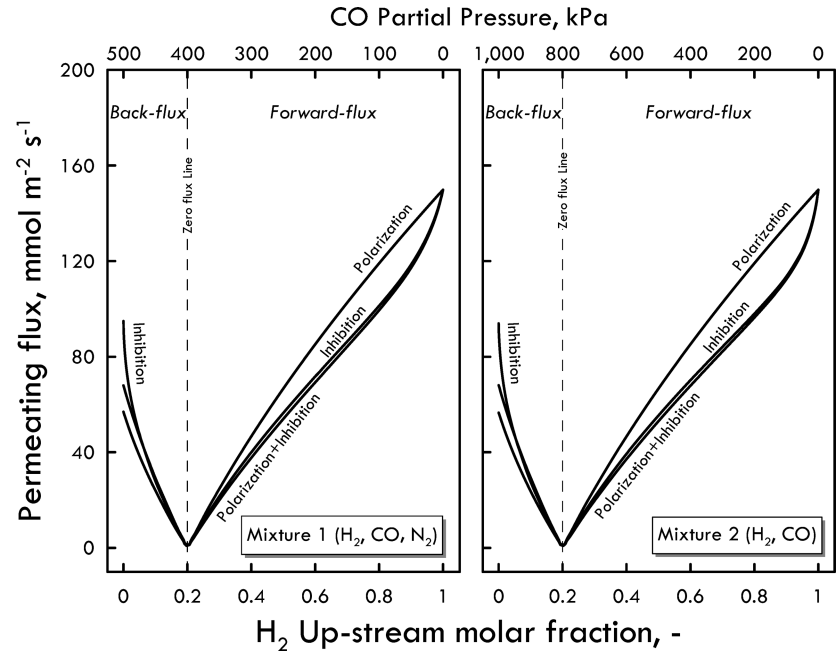

Figure 6. Hydrogen permeating flux as a function of H_2 upstream molar fraction for both mixtures. $P^{upstream} = 1000$ kPa and $P^{downstream} = 200$ kPa. The other operating conditions are reported in Table 7.

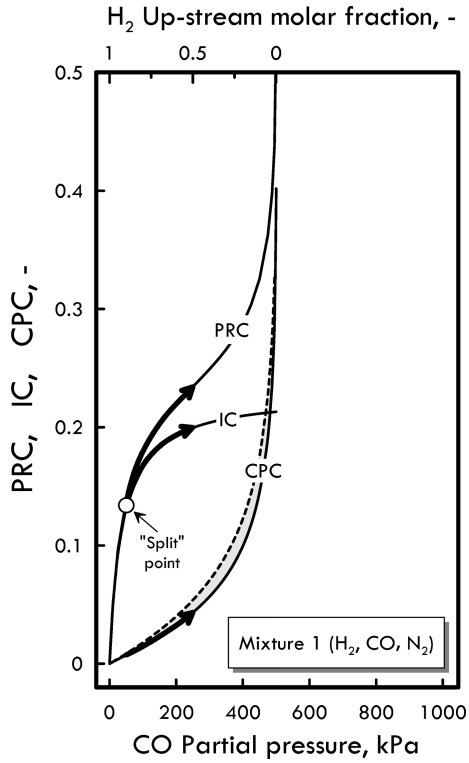

Figure 7. Permeation reduction, inhibition, and concentration polarization coefficient (PRC, IC, and CPC) as functions of CO partial pressure in the upstream for the mixture 1. The dashed line for CPC is evaluated in the absence of inhibition. $P^{upstream} = 1000$ kPa and $P^{downstream} = 200$ kPa. The other operating conditions are reported in Table 7.

on the other side, whereas the opposite situation occurs in the forward-flux. The net results of this phenomena favor the case where the membrane is used as hydrogen supplier with respect to the case where it is used as purifier. When the contributions of both inhibition and polarization are taken into account, another effect contributes to favoring the back-flux. In fact, in back-permeation mode, when the driving force is high enough, the CO partial pressure on the mixture side of the membrane is significantly moved away by the flux from the Pd-based surface to the bulk, reducing the negative effect of CO in this way.

4.3. Permeation Reduction Maps. A more direct quantification of inhibition and polarization can be provided in terms of here-named "permeation reduction maps", which refer to a "local" situation described above in Figure 1. These kinds of map can be very useful because they provide the amount of polarization, inhibition, and, therefore, overall permeation reduction as a function of the operating conditions. Additional significant efforts are required to find the appropriate correlations between the overall PRCs and the dimensionless parameters characterizing the fluid dynamics of the system: Reynolds (*Re*), Schmidt (*Sc*), and Sherwood (*Sh*) numbers.

This was already partially done in a previous paper (figures 8 and 9 in ref 7), where the coefficient CPC was evaluated at different *Re* numbers, but in this case, the situation is more complex because of the inhibition effect, and hence this topic requires another kind of analysis.

About the results obtained in this Article, Figure 7 shows the three reduction coefficients as functions of the CO partial pressure in the upstream side for mixture 1. The dashed line indicates the case in which no inhibition is accounted for, only polarization being therefore present. This curve is calculated in the same way as that shown in a previous work, where the presence of inhibition was not considered.[7] Here the separation paths (thicker arrows) are expressed in terms of these coefficients to highlight the fact that in the same unit very different conditions can occur according to the extent of the separation.

In fact, the more the hydrogen separated/purified, the higher the composition difference between inlet and outlet and thus the higher the influence of the external mass transfer and of inhibition, which are strongly related to each other. Following the sense of the separation paths, under conditions of high content of hydrogen, the polarization owing to both CO and N_2 does not provide an appreciable contribution. Therefore, dashed and solid lines are practically coincident, and the system is more sensitive to the CO content, showing an important influence in terms of inhibition, whose level increases significantly up to ~100 kPa, from which its profile goes toward a plateau value. Therefore, under these conditions, the system is driven by the inhibition phenomenon, and the overall PRC practically assumes the values of the IC. However, from 100 kPa on, the effect of the polarization begins to be relevant in such a way that PRC breaks away from the IC curve going toward the behavior of the polarization coefficient CPC.

Let us recall that the basic difference between the two phenomena (inhibition and polarization) is that the first one is limited by a thermodynamic equilibrium, whereas the second one can block, in principle, the overall permeation. For this reason, the slopes characterizing the curves of IC and CPC at a high CO content (right part of the curves) are opposite, being almost zero for the one of IC and very high as concerns CPC. In this sense, the "split" point shown by IC and PRC can be considered the lower limit of a range of conditions where the system is driven by both polarization and inhibition.

However, the fact that IC reaches a plateau does not mean that the inhibition effect is low compared with the one of polarization but rather that it has arrived at its maximum level after which the system cannot be affected by inhibition anymore. This consideration can lead up to developing a method to quantify separately the level of both inhibition and polarization effects, even whenever only CO and H_2 are present, the situation considered in mixture 2 (Figure 8). In fact, the case represented in Figure 8 clearly indicates that it is theoretically impossible to reach the plateau value by performing only permeation tests because after a certain level of CO, the polarization begins to be appreciable.

However, this effect is progressively lower as a higher membrane thickness is considered; therefore, the equilibrium value can be estimated with good approximation. The qualitative behavior of these curves is similar to the one of the plot in the previous Figure, but in this case, the tendency of IC toward the plateau is more evident because of the higher CO partial pressure. Furthermore, in both Figures, it is shown with more evidence what has been already seen when examining the permeance behavior (Figure 5), that is, that CPC with no inhibition is higher than CPC in its presence.

This aspect can also be directly visualized in Figure 9, where CPC is reported as a function of the hydrogen molar fraction at several total upstream pressures for both mixtures. Analogously to what was seen elsewhere,[7] CPC is a decreasing function of the hydrogen molar fraction in upstream, with the total pressure that favors the polarization due to the increased permeating flux. A novel result shown in this Figure regards the difference between the system affected by inhibition and the system without considering this phenomenon, that is, considering that CO increases only the external mass transfer resistance and does not affect the intrinsic membrane permeance (dashed lines in both the plots). This virtual case, which is shown at 1000 kPa

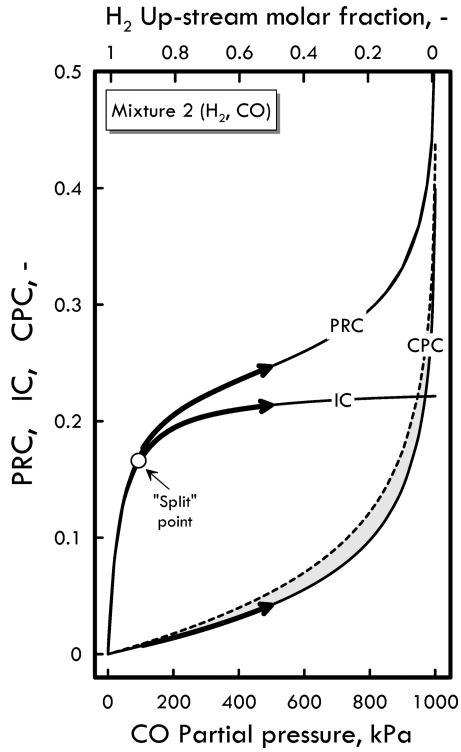

Figure 8. Permeation reduction, inhibition and concentration polarization coefficient (PRC, IC, and CPC) as functions of CO partial pressure in the upstream for the mixture 2. The dashed line for CPC is evaluated in the absence of inhibition. $P^{upstream} = 1000$ kPa and $P^{downstream} = 200$ kPa. The other operating conditions are reported in Table 7.

only to evidence that inhibition and polarization affect each other, clearly demonstrates that in presence of inhibitor the polarization decreases because of the reduced permeating flux.

From the CPC definition and from the results in the plots, it can be observed that the ratio of bulk and membrane permeance with inhibition is higher than this ratio measured without inhibition. Therefore, the reduction of the intrinsic permeance is more sensitive to the presence of inhibitors than the bulk one; this sensitivity difference tending to zero as the equilibrium value of the inhibitor content is progressively approached.

By analyzing the behavior of another indicator of the system performance, that is, the IC (Figure 10), it is shown that for both mixtures it increases continuously, approaching the equilibrium plateau due to the Sievert−Langmuir equation, by which the inhibition by CO has been dealt with in this Article. Analogously to what was done for the polarization coefficient, in this case, typical separation paths are indicated (thicker arrows at 400 kPa), showing that the inhibition phenomenon is progressively more significant as the purification process goes on (lower hydrogen content in mixture side). Concerning the dependence on total upstream pressure, it must be noticed that the higher the total pressure, the lower its effect.

This is the direct consequence of the interaction between inhibition and polarization, which is responsible for creating a CO partial pressure gradient in the mixture side along the permeation direction. However, this effect is progressively less important as the total pressure of mixture increases. To observe directly the overall effect of both polarization and inhibition by CO, the behavior of the previously defined PRC is shown in Figure 11 under the same conditions as those considered in Figures 9 and 10 as a function of H_2 and CO content for both mixtures. The reasons for the sigmoidal shape of the PRC curves have been already discussed previously in this section (Figures

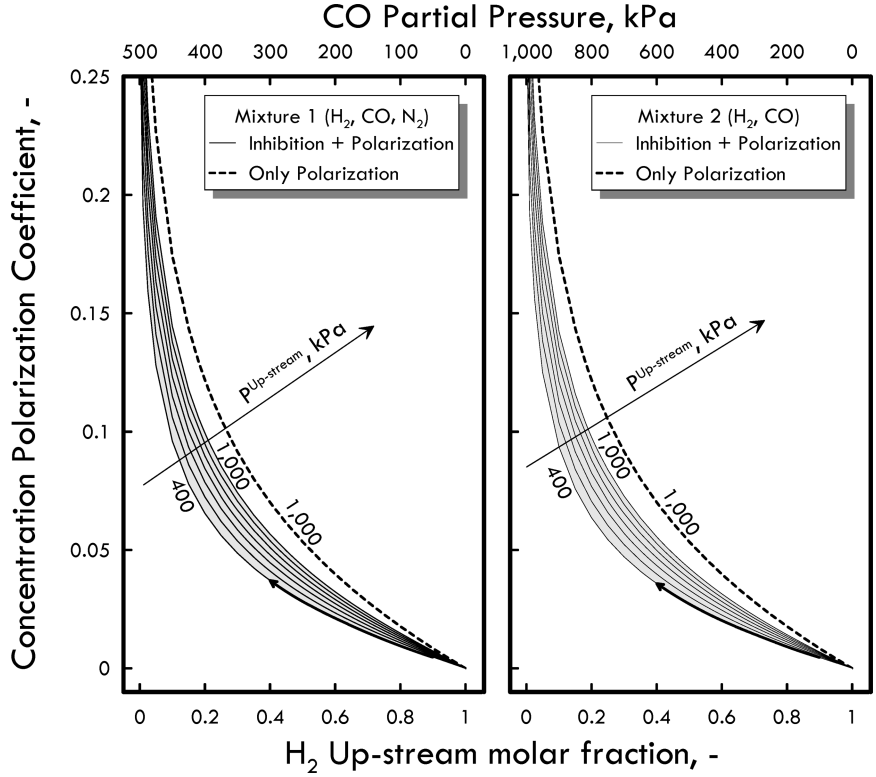

Figure 9. Concentration polarization coefficient (CPC) as functions of the H_2 upstream molar fraction for both mixtures. The separation paths are indicated only for the 400 kPa case The independent variable (hydrogen molar fraction) is reported in the main axis, whereas the corresponding CO partial pressure is indicated in the secondary axis just for convenience of the reader. $P^{upstream} = 1000$ kPa and $P^{downstream} = 200$ kPa. The other operating conditions are reported in Table 7.

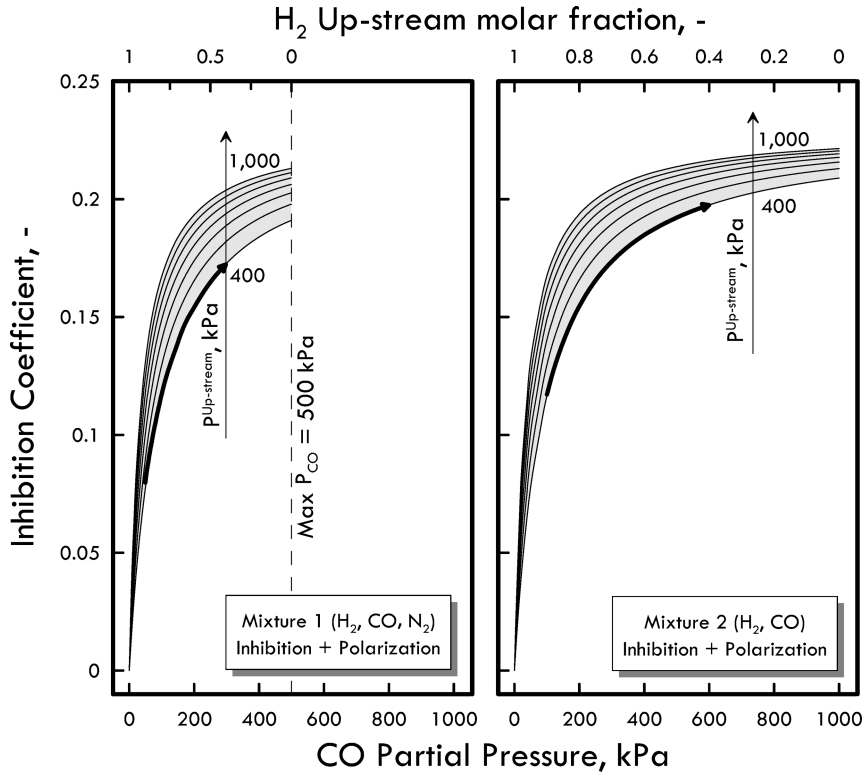

Figure 10. Inhibition coefficient (IC) as functions of the H_2 upstream molar fraction for both the mixtures. The separation paths are indicated only for the 400 kPa case. The independent variable (CO partial pressure) is reported in the main axis, whereas the corresponding hydrogen molar fraction is indicated in the secondary axis just for convenience of the reader. $P^{upstream} = 1000$ kPa and $P^{downstream} = 200$ kPa. The other operating conditions are reported in Table 7.

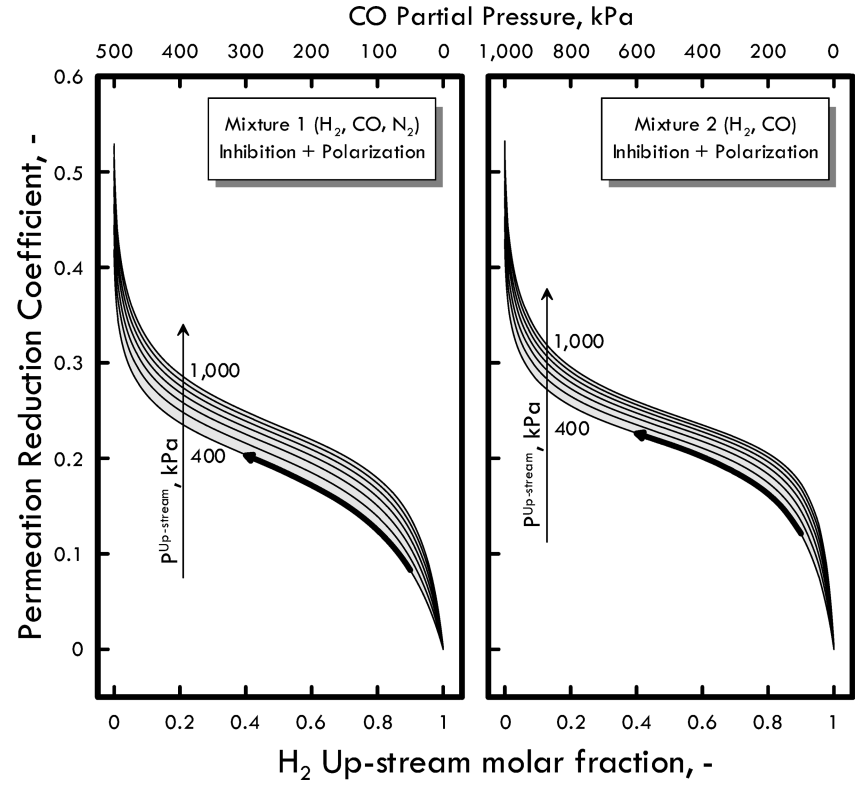

Figure 11. Permeation reduction coefficient (PRC) as functions of the H_2 upstream molar fraction for both mixtures. The separation paths are indicated only for the 400 kPa case. The independent variable (hydrogen molar fraction) is reported in the main axis, whereas the corresponding CO partial pressure is indicated in the secondary axis just for convenience of the reader. $P^{upstream} = 1000$ kPa and $P^{fownstream} = 200$ kPa. The other operating conditions are reported in Table 7.

7 and 8), where it has been highlighted that PRC assumes the characteristic shape of CPC or IC in dependence on the mixture content in terms of H_2 and CO. Therefore, also for this coefficient, the effect of the total pressure is progressively less appreciable, becoming negligible from about 1000 kPa on. However, considering that the flux progressively increases with the total pressure (higher driving force), it is possible to conclude that the most convenient operating conditions to reduce the effect of the permeation reduction in a membrane-based separation/purification system are established at high total pressure.

6. Conclusions

In this work, the influence of inhibition by CO and concentration polarization on hydrogen permeation through Pd-based membranes was investigated by means of a novel overall PRC, which takes into account the permeance decrease with respect to intrinsic value. The membrane behavior was analyzed by the here-called "permeation reduction maps", where the above-mentioned coefficients were calculated under several operating conditions (hydrogen molar fraction, CO partial pressure in mixture, and total pressure of upstream) as well as an IC and CPC. The usefulness of this analysis consisted of the possibility of using Sieverts law even when the membrane is affected by negative factors like polarization and inhibition by CO. Therefore, the effective permeance, which represents the actual main design variable, can be evaluated by reading the overall PRC directly on the permeation reduction maps, which have been built for some operating conditions. The whole investigation was performed by developing a new model obtained from modifying and merging two approaches that consider inhibition and polarization separately. From this analysis, it was observed that the inhibition by CO prevails on the polarization (at high hydrogen molar fraction), which begins to be appreciable at lower hydrogen contents, where the CO influence (modeled by Sievert−Langmuir equation) approaches the equilibrium value. In conclusion, Sieverts law can still be used by integrating in its original form an additional term (PRC) accounting for polarization and inhibition, which requires the use of the PRC maps developed in this work.

Appendix

Symbols

D_H^0	pre-exponential factor of the atomic hydrogen diffusion coefficient [$m^2\ s^{-1}$]
E_d	activation energy of the atomic hydrogen diffusion coefficient [J mol^{-1}]
K	probability parameter in eq 3
K_{CO}	Langmuir equilibrium constant in eq 9
k_D	desorption kinetic constant in eq 4 [$m^2\ mol_{Pd}^{-1}\ s^{-1}$]
M_{H_2}	hydrogen molar mass [kg mol^{-1}]
N_A, N_O	superficial concentration of sites occupied by atomic hydrogen [$mol_H\ m^{-2}$], [$mol_O\ m^{-2}$]
N_{AA}	superficial concentration of pairs of sites occupied by atomic hydrogen [$mol_H\ m^{-2}$]
N_S	total superficial concentration of free sites [$mol_{Pd}\ m^{-2}$]
N_b	total bulk concentration of free sites [$mol_{Pd}\ m^{-3}$]
P	pressure [Pa]
r	net rate [$mol_H\ m^{-2}\ s^{-1}$] (Table 1)
R_i^{net}	specific net rate [$mol_H\ m^{-2}\ s^{-1}$] (Table 2)
R_g	ideal gas constant [J $mol^{-1}\ K^{-1}$]
Re	Reynolds' number
S_0	sticking coefficient for a Pd-clean surface
T	temperature [K]
x	molar fraction

Greek Symbols

α	Langmuir parameter in eq 9
β	kinetic constant in eq 5 [$m^3\ mol_{Pd}^{-1}\ s^{-1}$]
δ	thickness [m]
ν	kinetic constant in eq 6 [$m^3\ mol_{Pd}^{-1}\ s^{-1}$]
θ	surface coverage due to atomic hydrogen
θ_{OO}	surface coverage of empty pairs of sites
ξ	atomic hydrogen concentration in Pd-bulk, [mol_H/mol_{Pd}]
π	permeance [mol $m^{-2}\ s^{-1}\ Pa^{-0.5}$]

Acronyms

CPC	concentration polarization coefficient
IC	inhibition coefficient
PRC	permeation reduction coefficient
DF	Sieverts driving force [$Pa^{0.5}$]

References and Notes

(1) Morreale, B. D.; Ciocco, M. V.; Enick, R. M.; Morsi, B. I.; Howard, B. H.; Cugini, A. V.; Rothenberger, K. S. The Permeability of Hydrogen in Bulk Palladium at Elevated Temperatures and Pressures. *J. Membr. Sci.* **2003**, *212*, 87–97.

(2) Ciocco, M. V.; Morreale, B. D.; Rothenberger, K. S.; Howard, B. H.; Cugini, A. V.; Killmeyer, R. P.; Enick, R. M. High-Pressure, High-Temperature Hydrogen Permeability Measurements of Supported Thin-Film Palladium Membranes. Proceedings of the 19th International Pittsburgh Coal Conference, Sept 24−26, 2002, Pittsburgh, PA; paper no. 49-3.

(3) EG&G Technical Services, Inc. *Fuel Cell Handbook*, 7th ed.; U.S. Department of Energy, Office of Fossil Energy, National Energy Technology Laboratory: Morgantown, WV, 2004.

(4) *Modeling of Process Intensification*; Keil, J. K., Ed.; Wiley-VCH: Weinheim, Germany, 2007.

(5) Dittmeyer, R.; Höllein, V.; Daub, K. Membrane Reactors for Hydrogenation and Dehydrogenation Processes Based on Supported Palladium. *J. Mol. Catal A: Chem.* **2001**, *173*, 135–184.

(6) Caravella, A.; Barbieri, G.; Drioli, E. Modelling and Simulation of Hydrogen Permeation through Supported Pd-Based Membranes with a Multicomponent Approach. *Chem. Eng. Sci.* **2008**, *63*, 2149–2160.

(7) Caravella, A.; Barbieri, G.; Drioli, E. Concentration Polarization Analysis in Self-Supported Pd-Based Membranes. *Sep. Purif. Technol.* **2009**, *66*, 613–624.

(8) He, G.; Mi, Y.; Yue, P. L.; Chen, G. Theoretical Study on Concentration Polarization in Gas Separation Membrane Processes. *J. Membr. Sci.* **1999**, *153*, 243–258.

(9) Lüdtke, O.; Behling, R. D.; Ohlrogge, K. Concentration Polarization in Gas Permeation. *J. Membr. Sci.* **1998**, *146*, 145–157.

(10) Peters, T. A.; Stange, M.; Klette, H.; Bredesen, R. High-Pressure Performance of Thin Pd−23%Ag/stainless steel Composite Membranes in Water Gas Shift Gas Mixtures; Influence of Dilution, Mass Transfer and Surface Effects on the Hydrogen Flux. *J. Membr. Sci.* **2008**, *316*, 119–127.

(11) Zhang, J.; Liu, D.; He, M.; Xu, H.; Li, W. Experimental and Simulation Studies on Concentration Polarization in H_2 Enrichment by Highly Permeable and Selective Pd Membranes. *J. Membr. Sci.* **2006**, *274*, 83–91.

(12) Haraya, K.; Hakuta, T.; Yoshitome, H. A study of concentration polarization phenomenon on the surface of a gas separation membrane. *Sep. Sci. Technol.* **1987**, *22*, 1425–1438.

(13) Takaba, H.; Nakao, S. Computational Fluid Dynamics Study on Concentration Polarization in H_2/CO Separation Membranes. *J. Membr. Sci.* **2005**, *249*, 83–88.

(14) Gielens, F. C.; Tong, H. D.; Vorstman, M. A. G.; Keurentjes, J. T. F. Measurement and Modeling of Hydrogen Transport through High-Flux Pd Membranes. *J. Membr. Sci.* **2007**, *289*, 15–25.

(15) Guazzone, F.; Engwall, E. E.; Ma, Y. H. Effects of Surface Activity, Defects and Mass Transfer on Hydrogen Permeance. *Catal. Today* **2006**, *118*, 24–31.

(16) Mejdell, A. L.; Klette, H.; Ramachandran, A.; Borg, A.; Bredesen, R. Hydrogen Permeation of Thin, Free-Standing Pd/Ag23% Membranes before and after Heat Treatment in Air. *J. Membr. Sci.* **2008**, *307*, 96–104.

(17) Mejdell, A. L.; Jondahl, M.; Peters, T. A.; Bredesen, R.; Venvik, H. J. Effects of CO and CO_2 on Hydrogen Permeation through a ∼3 μm Pd/Ag 23 wt % Membrane Employed in a Microchannel Membrane Configuration. *Sep. Purif. Technol.* **2009**, *68*, 178–184.

(18) Mejdell, A. L.; Chen, D.; Peters, T. A.; Bredesen, R.; Venvik, H. J. The Effect of Heat Treatment in Air on CO Inhibition of a ~3 μm Pd−Ag (23 wt %) Membrane. *J. Membr. Sci.* **2010**, *350*, 371–377.

(19) Roa, F.; Way, J. D. the Effect of Air Exposure on Palladium−Copper Composite Membranes. *Appl. Surf. Sci.* **2005**, *240*, 85.

(20) Uchikawa, H.; Okazaki, T.; Sato, K. New Technique of Activating Palladium Surface for Absorption of Hydrogen or Deuterium. *Jpn. J. Appl. Phys.* **1993**, *32*, 5095 (part 1, no. 11A).

(21) Wang, D.; Clewley, J. D.; Flanagan, T. B.; Balasubramaniam, B.; Shanahan, K. L. Enhanced Rates of Hydrogen Adsorption Resulting from Oxidation of Pd or Internal Oxidation of Pd−Al alloys. *J. Alloys Compd.* **2000**, *298*, 261.

(22) Ertl, G.; Koch, J. Adsorption Studies with a Pd(111) Surface. In *Adsorption−Desorption Phenomena: Proceedings of the II International Conference Held at Florence in April 1971*; Ricca, F., Ed.; Academic Press: London, 1972; pp 345−357.

(23) Conrad, H.; Ertl, G.; Koch, J.; Latta, E. E. Adsorption of CO on Pd Single Crystal Surfaces. *Surf. Sci.* **1974**, *43*, 462–480.

(24) Davies, P. W.; Lambert, R. M. Structural Influences on the Adsorption-Desorption Properties of the Palladium/CO System. *Surf. Sci.* **1981**, *111*, L671−L674.

(25) Prigge, D.; Schlenk, W.; Bauer, E. The Adsorption of CO and O_2 on Ultrathin Pd Layers on W(110). *Surf. Sci.* **1982**, *123*, L698−L702.

(26) Ortega, A.; Huffman, F. M.; Bradshaw, A. M. The Adsorption of CO on Pd(100) Studied by IR Reflection Absorption Spectroscopy. *Surf. Sci.* **1982**, *119*, 79–94.

(27) Hara, S.; Sakaki, K.; Itoh, N. Decline in Hydrogen Permeation Due to Concentration Polarization and CO Hindrance in a Palladium Membrane Reactor. *Ind. Eng. Chem. Res.* **1999**, *38*, 4913–4918.

(28) Barbieri, G.; Scura, F.; Lentini, F.; De Luca, G.; Drioli, E. A Novel Model Equation for the Permeation of Hydrogen in Mixture with Carbon Monoxide through Pd-Ag Membranes. *Sep. Purif. Technol.* **2008**, *61*, 217–224.

(29) Scura, F.; Barbieri, G.; De Luca, G.; Drioli, E. The Influence of the CO Inhibition Effect on the Estimation of the H_2 Purification Unit Surface. *Int. J. Hydrogen Energy* **2008**, *33*, 4183–4192.

(30) Barbieri, G.; Brunetti, A.; Tricoli, G.; Drioli, E. An Innovative Configuration of a Pd-Based Membrane Reactor for the Production of Pure Hydrogen. Experimental Analysis of Water Gas Shift. *J. Power Sources* **2008**, *182*, 160–167.

(31) King, D. A.; Wells, M. G. Reaction Mechanism in Chemisorption Kinetics: Nitrogen on the {1 0 0} Plane of Tungsten. *Proc. R. Soc. London, Ser. A* **1974**, *339*, 245.

(32) Behm, R. J.; Christmann, K.; Ertl, G. Adsorption of Hydrogen on Pd (1 0 0). *Surf. Sci.* **1980**, *99*, 320.

(33) Ward, T.; Dao, T. Model of Hydrogen Permeation Behaviour in Palladium Membranes. *J. Membr. Sci.* **1999**, *153*, 211–231.

(34) Oriani, R. A. The Physical and Metallurgical Aspects of Hydrogen in Metals. In *ICCF4, Fourth International Conference on Cold Fusion*; Electric Power Research Institute: Palo Alto, CA, 1993.

JP104767Q